ACS Sustainable Chemistry & Engineering

Letter

pubs.acs.org/journal/ascecg

Preparation of Single-Walled Carbon Nanotubes from Fullerene Waste Soot

Chao Hu, Chang Yu, Mingyu Li, Xiaoming Fan, Juan Yang, Peng Zhang, Shiyao Wang, Zongbin Zhao, and Jieshan Qiu*

Carbon Research Laboratory, Liaoning Key Lab for Energy Materials and Chemical Engineering, State Key Lab of Fine Chemicals, School of Chemical Engineering, Dalian University of Technology, Dalian 116024, China

ABSTRACT: Single-walled carbon nanotubes (SWCNTs) were successfully prepared from fullerene waste soot (FWS) by the arc discharge method in a helium atmosphere. The yield of the as-prepared SWCNTs reached as high as 6 g/h, indicating a great potential for further large scale production. FWS-based SWCNTs were systematically examined using scanning electron microscopy, transmission electron microscope, high-resolution transmission electron microscopy, and Raman spectroscopy. The results show that the as-obtained SWCNTs have an extraordinary crystalline integrity with a diameter of 1.2−2.2 nm. Compared with the SWCNTs synthesized from graphite under the same experimental conditions, it was found that FWS as feedstock for synthesis of SWCNTs was more efficient due to its higher reactivity in the electric arc discharge environment. The possible mechanism involved in the formation process of SWCNTs from FWS is proposed and discussed in terms of its turbostratic structure with pentagonal defects and the process parameters adopted in the study.

KEYWORDS: *Single-walled carbon nanotubes, Fullerene waste soot, Byproduct, Arc discharge, Pentagonal defect*

INTRODUCTION

Single-walled carbon nanotubes (SWCNTs), a single layer of graphene rolled up, have received a great deal of attention and have been widely used in many different applications, such as transistors,[1] supercapacitors,[2] sensors,[3] field emitters,[4] and photovoltaic devices,[5] because of their exceptional electrical, mechanical, physical, and chemical properties.[6−9] Up to now, various methods have been developed for the synthesis of SWCNTs, such as arc discharge,[10] laser ablation,[11] catalytic chemical vapor deposition,[12] etc. Of these available methods, it is believed that the arc discharge method is an efficient method for the synthesis of SWCNTs due to its low cost and simplicity as well as its capability of making high quality SWCNTs with perfect structures. In the past two decades, great progress has been made on the synthesis of SWCNTs by the arc discharge method. Journet et al. successfully obtained SWCNTs on a large scale from graphite with a mixture of 1% yttrium and 4.2% nickel as the catalyst, and the content of SWCNTs in the collected deposits was about 80%.[10] Cheng et al. designed a novel reactor with a rotatable cylinder anode for semi-continuous synthesis of SWCNTs in a hydrogen buffer gas, indicating a promising approach for the commercial-scale synthesis of SWCNTs.[13] Zhang et al. reported a facile method for diameter-selective synthesis of SWCNTs, in which a weak magnetic field being perpendicular to the electric field was applied to the arc plasma in the interelectrode gap.[14,15] In addition, other studies focused on the experimental conditions that affect the synthesis of SWCNTs in the arc discharge process, such as the catalyst,[16−20] buffer gas with specified pressure,[21,22] carbon structure of the anode,[23−27] and gravity of the Earth.[28] In spite of the above-mentioned endeavors, large-scale production of SWCNTs with high quality from cheap carbon sources is still highly desired.

Fullerene waste soot (FWS) is the main byproduct in the production of fullerenes by arc discharge or flames[29] and can be produced with a capacity of more than tens of tons per year. Nevertheless, how to further recycle this cheap and valuable resource still remains a challenge. Egashira et al. first explored the possibility for utilizing a toluene-insoluble fraction of fullerene soot as an electrode in a electrical double-layer capacitor.[30] Following Egashira's work, Spassova and his co-workers demonstrated that FWS could be used as a catalyst support in low-temperature reduction of NO in the presence of CO.[31] In the present work, we first report the synthesis of high quality SWCNTs using FWS as the starting material by the arc discharge method. The yield of the as-prepared product was improved in comparison to that from graphite. This will lead to new possibilities for making carbon materials with different structures using FWS as the carbon source.

EXPERIMENTAL SECTION

All chemicals used were of ultrapure analytical grade. The experimental setup is basically the same as that reported previously.[13] For a typical run, FWS (Jing Meng Hi-Tech Corp.) was mixed with Ni powders and Y_2O_3 in a weight ratio of 10:2:1. The mixture was pressed in a mold

Special Issue: Sustainable Chemical Product and Process Engineering

Received: September 9, 2013
Revised: September 29, 2013
Published: October 4, 2013

   dx.doi.org/10.1021/sc4003278 | *ACS Sustainable Chem. Eng.* 2014, 2, 14−18

and carbonized at 900 °C for 5 h to produce conductive and self-supporting carbon cylinders with a diameter of 25 mm. In the arc discharge experimental process, carbon cylinders were placed on a water-cooled copper platform that served as the anode, and an upper high-purity graphite rod was used as the cathode. The arc discharge was conducted at a current of about 100 A in a helium atmosphere at 50 kPa. For comparison, graphite powders were also used as the carbon feedstock to synthesize SWCNTs under the same operational conditions mentioned above.

Morphologies and structures of the as-prepared SWCNTs were analyzed by scanning electron microscopy (SEM, JEOL JSM-5600LV), transmission electron microscopy, and high-resolution transmission electron microscopy (TEM and HRTEM, Philips Tecnai G^2 20). The Raman spectra of the SWCNTs derived from FWS and graphite were both recorded with a Jobin Yvon LabRam HR800 spectrometer at room temperature (He−Ne laser, 632.8 nm). The X-ray diffraction (XRD) was recorded on a Rigaku D/MAX 2400 diffractometer equipped with a Cu Kα X-ray source operated at 40 kV and 50 mA.

RESULTS AND DISCUSSION

The web-like substances hanging from the upper chamber wall and thin films on the inner chamber wall are involved in the reactor, and these materials have a rubbery texture and can be peeled away in strips. The detailed microtopographies and microstructures are shown in Figure 1. From the typical SEM image shown in Figure 1a, it can be found that a large number of filament-like SWCNTs are intertwined to form a macroscopic network architecture, and some deposits that are made up of catalyst nanoparticles surrounded by amorphous carbon are present in the network or on the surface of the SWCNTs architecture, which is clearly observed by low-resolution TEM image shown in Figure 1b. The SWCNTs usually tend to aggregate in the form of bundles (Figure 1c), which is believed to be due to the existing van der Waals interaction between the nanotubes.[32] HRTEM images further reveal that the FWS-based SWCNTs have a high crystalline integrity, and the diameter of the SWCNTs ranges from 1.2 to 2.0 nm (see Figure 1d for an example). It is worth noting that the ends of the SWCNTs are capped by hemispherical carbon, as indicated in Figure 1e.

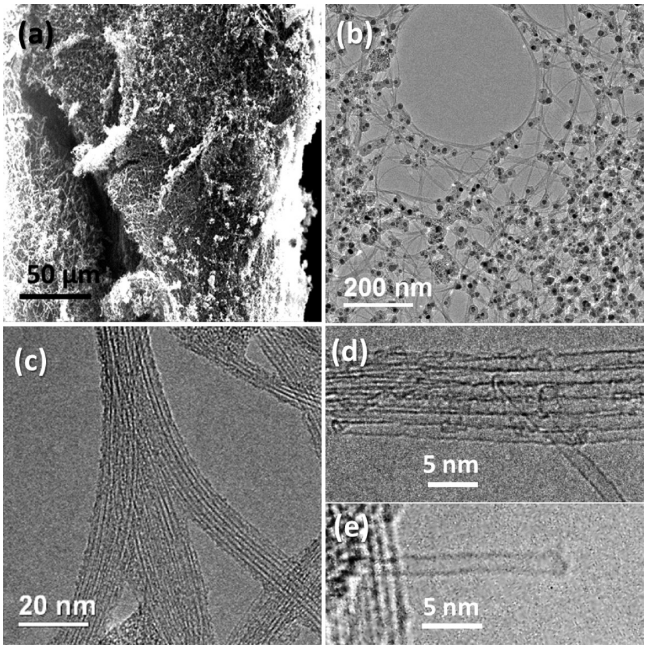

Figure 1. Low magnification SEM image (a), TEM images (b, c), and HRTEM images (d, e) of the as-obtained SWCNTs from FWS.

For comparison, graphite powders were also utilized as a carbon source to synthesize SWCNTs under the same conditions. The result shows that the as-obtained products from the FWS and graphite powders are similar in morphology. However, more than 1 g of SWCNTs was achieved from FWS (denoted as SWCNTs-F) within 10 min, twice as much in comparison to the product obtained from graphite powders (denoted as SWCNTs-G). This may be attributed to the differences in initial types and energies of carbon species vaporized from FWS and graphite that derive from their different bonding environments. The amorphous structure of FWS rather than the perfect crystallinity of graphite is more easily broken in the electric arc discharge environment, and fullerene-like fragments involved in FWS may be directly utilized as "seeds" for the growth of SWCNTs.

Raman spectroscopy is a powerful tool that is capable of yielding more detailed information about the SWCNTs' structure,[33] in which two typical bands for graphite materials are present: the so-called G band located at 1592 cm^{-1}, which is related to the vibration of sp^2 bonded carbon atoms in a hexagonal graphite lattice, and the so-called D band located at 1295−1300 cm^{-1}, which is associated with disordered carbons. The relative intensity ratio of the D and G bands (I_D/I_G) is indicative of the degree of carbon graphitization. Figure 2 shows typical Raman spectra of SWCNTs-F and SWCNTs-G in the range of 20−2000 cm^{-1}, in which the I_D/I_G of the SWCNTs-F and SWCNTs-G are calculated to be 0.12 and 0.16, respectively, revealing that the SWCNTs-F are graphitized and have a crystalline integrity comparable to that of graphite. The lower Raman shift around 110−190 cm^{-1} is caused by the radial breathing mode (RBM peak) of SWCNTs, which is related to the diameters of the SWCNTs. As shown in the inset of Figure 2, the similar peaks can be observed for SWCNTs-F and SWCNTs-G samples, and two peaks at 162 cm^{-1} and 168 cm^{-1} are strikingly visible, indicating that the diameters of SWCNTs do not vary with the type of carbon source. This also implies that the structure of carbon source has little influence on the diameter of SWCNTs in the present work.

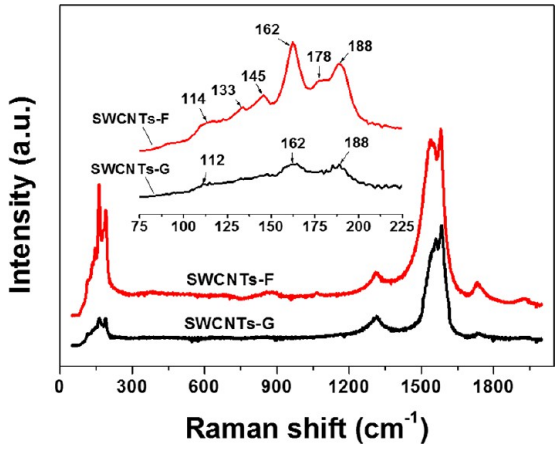

Figure 2. Raman spectra of the as-obtained SWCNTs from two different carbon feedstocks.

From the Raman spectra of RBM, the diameters of the SWCNTs can be calculated using a formula of $\omega = 238/d^{0.93}$, in which ω and d are defined as the RBM frequency and tube

dx.doi.org/10.1021/sc4003278 | ACS Sustainable Chem. Eng. 2014, 2, 14−18

diameter, respectively.[34] The calculated diameters of SWCNTs from the RBM frequency are in the range of 1.20−2.20 nm, which is in a good agreement with that observed in the HRTEM images discussed above.

In order to understand the formation mechanism of SWCNTs-F, the starting material of the FWS and FWS-derived anode are also characterized by TEM and XRD techniques, respectively. The TEM image in Figure 3a shows that the FWS

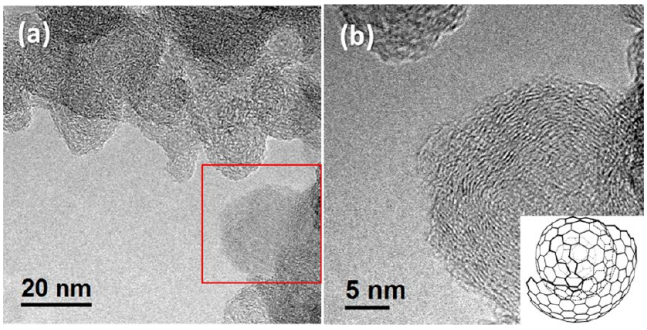

Figure 3. Typical TEM (a) and HRTEM (b) of raw FWS.

sample is an aggregate of a semi-spherical carbon onion-like structure, and its diameter changes in the range of 5−20 nm. Another HRTEM image of FWS in Figure 3b reveals a spheroidal graphitic nanoparticle with a diameter of about 20 nm, built by concentric carbon layers around a defect fullerene nucleus. This positive curvature of the graphene structure is formed by the insertion of a large amount of defects such as pentagons that are highly active. The XRD pattern of the FWS-derived anode is shown in Figure 4, where a broad peak

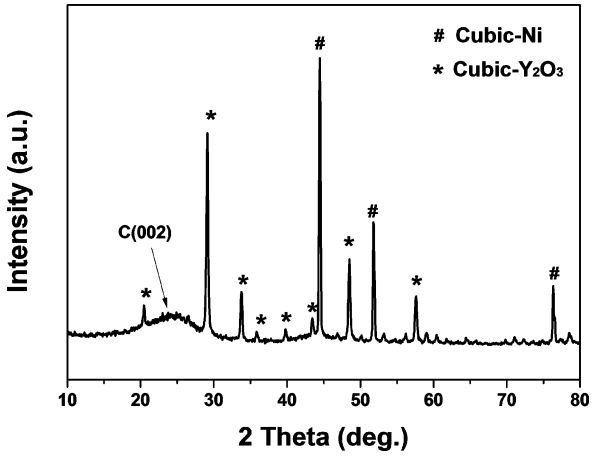

Figure 4. XRD pattern of the anode prepared from FWS.

corresponding to the diffraction of (002) graphite planes is clearly visible, indicating that turbostratic stacking of carbon layers is dominant in the FWS. The structure of the turbostratic stacking of the FWS carbon layers with a large number of defects may be highly active, which will make the FWS-derived anode easier and faster than that of graphite to vaporize to form the carbon species for the growth of SWCNTs in the arc discharge process. In addition, a series of sharp diffraction peaks originated from cubic Ni and Y_2O_3 could also be found in the XRD pattern of the anode (Figure 4). These two components are introduced and used as catalysts for the synthesis of SWCNTs.

On the basis of the discussion above, a growth model of SWCNTs involved in the arc discharge process is proposed, and the schematic is shown in Figure 5. In the first step, the

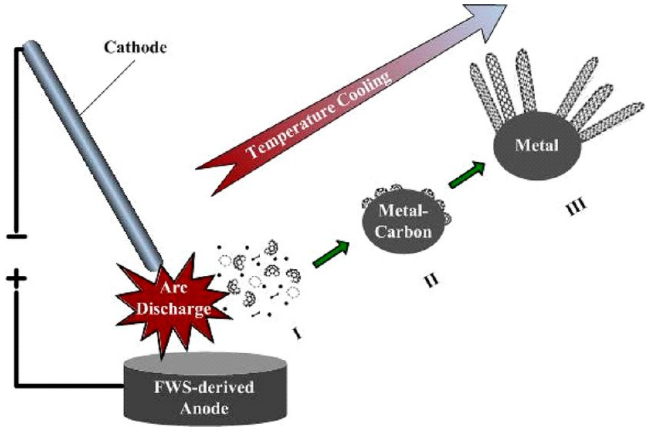

Figure 5. Illustration of the growth model of SWCNTs from FWS.

carbon species, mainly excited atoms and small clusters, are vaporized to form a plasma zone and begin to aggregate immediately and form fullerene-like pentagonal ring-rich fragments. Compared with the 2D structure of graphite, FWS as a quasi-0D structure has more tensile strength due to the curvature of pentagon defects on the carbon onion structures, so the FWS-derived anode is relatively more reactive and easier to vaporize into a variety of reactive species. Moreover, FWS is more likely to form fullerene-like fragments that are considered the "seeds" for the growth of SWCNTs because of a better microstructure compatibility.[35,36] The metal atoms exist in the form of gas phase at this stage (step I). However, as the temperature further decreases, the metal atoms condense to form particles or droplets and are gradually supersaturated by carbon (step II). The "open edges" of the fullerene-like fragments tend to stick to the metal particles to eliminate dangling bonds and act as precursors for the SWCNTs growth. When the temperature is close to the eutectic temperature, SWCNTs begin to grow using the carbon species supplied by precipitation from the metal particles or amorphous carbon that surrounds the metal particles (step III). With the information discussed above, it can be concluded that a precursor with a fullerene-like structure is the dominating or leading factor determining the formation of the SWCNTs. It has also been confirmed by Zhang[37] that SWCNTs can be produced by laser ablation at a much lower temperature of 400 °C when using fullerene powder as the carbon source. In contrast, no SWCNTs were found in the product ablated from the pure graphite target at such a temperature.

CONCLUSIONS

In summary, high quality SWCNTs have been successfully synthesized from FWS in large scale by the arc discharge method in the presence of Y_2O_3/Ni catalysts in a helium atmosphere, in which the carbon source is a dominating factor for determining the features and yield of SWCNTs. Compared with graphite, FWS as the starting material to produce SWCNTs results in a higher yield due to its turbostratic stacking of carbon layers and curly structure with lots of pentagonal defects. This provides an effective way to produce SWCNTs with high quality using FWS as the carbon source

dx.doi.org/10.1021/sc4003278 | ACS Sustainable Chem. Eng. 2014, 2, 14−18

and to realize the utilization of byproduct FWS. Nevertheless, more detailed work needs to be explored in the future.

AUTHOR INFORMATION

Corresponding Author

*E-mail: jqiu@dlut.edu.cn. Fax: +86-411-84986080.

Notes

The authors declare no competing financial interest.

ACKNOWLEDGMENTS

This work was partly supported by NSFC (U1203292) and the Specialized Research Fund for the Doctoral Program of Higher Education of China (20120041110020).

REFERENCES

(1) Tans, S. J.; Devoret, M. H.; Dai, H.; Thess, A.; Smalley, R. E.; Geerligs, L. J.; Dekker, C. Individual single-wall carbon nanotubes as quantum wires. *Nature* **1997**, *386* (6624), 474−477.

(2) An, K. H.; Kim, W. S.; Park, Y. S.; Choi, Y. C.; Lee, S. M.; Chung, D. C.; Bae, D. J.; Lim, S. C.; Lee, Y. H. Supercapacitors using single-walled carbon nanotube electrodes. *Adv. Mater.* **2001**, *13* (7), 497−500.

(3) Li, J.; Lu, Y.; Ye, Q.; Cinke, M.; Han, J.; Meyyappan, M. Carbon nanotube sensors for gas and organic vapor detection. *Nano Lett.* **2003**, *3* (7), 929−933.

(4) de Heer, W. A.; Châtelain, A.; Ugarte, D. A carbon nanotube field-emission electron source. *Science* **1995**, *270* (5239), 1179−1180.

(5) Kymakis, E.; Amaratunga, G. A. J. Single-wall carbon nanotube/conjugated polymer photovoltaic devices. *Appl. Phys. Lett.* **2002**, *80* (1), 112−114.

(6) Iijima, S.; Ichihashi, T. Single-shell carbon nanotubes of 1-nm diameter. *Nature* **1993**, *363* (6430), 603−605.

(7) Bethune, D. S.; Kiang, C. H.; Devries, M. S.; Gorman, G.; Savoy, R.; Vazquez, J.; Beyers, R. Cobalt-catalysed growth of carbon nanotubes with single-atomic-layer. *Nature* **1993**, *363* (6430), 605−607.

(8) Wong, E. W.; Sheehan, P. E.; Lieber, C. M. Nanobeam mechanics: Elasticity, strength, and toughness of nanorods and nanotubes. *Science* **1997**, *277* (5334), 1971−1975.

(9) Ouyang, M.; Huang, J. L.; Lieber, C. M. Fundamental electronic properties and applications of single-walled carbon nanotubes. *Acc. Chem. Res.* **2002**, *35* (12), 1018−1025.

(10) Journet, C.; Maser, W. K.; Bernier, P.; Loiseau, A.; delaChapelle, M. L.; Lefrant, S.; Deniard, P.; Lee, R.; Fischer, J. E. Large-scale production of single-walled carbon nanotubes by the electric-arc technique. *Nature* **1997**, *388* (6644), 756−758.

(11) Guo, T.; Nikolaev, P.; Thess, A.; Colbert, D. T.; Smalley, R. E. Catalytic growth of single-walled nanotubes by laser vaporization. *Chem. Phys. Lett.* **1995**, *243* (1−2), 49−54.

(12) Hafner, J. H.; Bronikowski, M. J.; Azamian, B. R.; Nikolaev, P.; Rinzler, A. G.; Colbert, D. T.; Smith, K. A.; Smalley, R. E. Catalytic growth of single-wall carbon nanotubes from metal particles. *Chem. Phys. Lett.* **1998**, *296* (1−2), 195−202.

(13) Liu, C.; Cong, H. T.; Li, F.; Tan, P. H.; Cheng, H. M.; Lu, K.; Zhou, B. L. Semi-continuous synthesis of single-walled carbon nanotubes by a hydrogen arc discharge method. *Carbon* **1999**, *37* (11), 1865−1868.

(14) Su, Y.; Zhang, Y.; Wei, H.; Zhang, L.; Zhao, J.; Yang, Z.; Zhang, Y. Magnetic-field-induced diameter-selective synthesis of single-walled carbon nanotubes. *Nanoscale* **2012**, *4* (5), 1717−1721.

(15) Su, Y.; Zhang, Y.; Wei, H.; Yang, Z.; Kong, E. S.-W.; Zhang, Y. Diameter-control of single-walled carbon nanotubes produced by magnetic field-assisted arc discharge. *Carbon* **2012**, *50* (7), 2556−2562.

(16) Yao, M. G.; Liu, B. B.; Zou, Y. G.; Wang, L.; Li, D. M.; Cui, T.; Zou, G. T.; Sundqvist, B. Synthesis of single-wall carbon nanotubes and long nanotube ribbons with Ho/Ni as catalyst by arc discharge. *Carbon* **2005**, *43* (14), 2894−2901.

(17) Yao, M. G.; Liu, B. B.; Zou, Y. G.; Wang, L.; Cui, T.; Zou, G. T.; Li, J. X.; Sundqvist, B. Effect of rare-earth component of the RE/Ni catalyst on the formation and nanostructure of single-walled carbon nanotubes. *J. Phys. Chem. B* **2006**, *110* (31), 15284−15290.

(18) He, D. L.; Liu, Y. N.; Zhao, T. K.; Zhu, J. W.; Yu, G. Effect of metal oxide and oxygen on the growth of single-walled carbon nanotubes by electric arc discharge. *J. Nanopart. Res.* **2008**, *10* (3), 409−414.

(19) Wang, H. F.; Li, Z. H.; Inoue, S.; Ando, Y. Influence of Mo on the growth of single-walled carbon nanotubes in arc discharge. *J. Nanosci. Nanotechnol.* **2010**, *10* (6), 3988−3993.

(20) Huang, L.; Wu, B.; Chen, J.; Xue, Y.; Liu, Y.; Kajiura, H.; Li, Y. Synthesis of single-walled carbon nanotubes by an arc-discharge method using selenium as a promoter. *Carbon* **2011**, *49* (14), 4792−4800.

(21) Makita, Y.; Suzuki, S.; Kataura, H.; Achiba, Y. Synthesis of single wall carbon nanotubes by using arc discharge technique in nitrogen atmosphere. *Eur. Phys. J. D* **2005**, *34* (1−3), 287−289.

(22) Hinkov, I.; Farhat, S.; Scott, C. D. Influence of the gas pressure on single-wall carbon nanotube formation. *Carbon* **2005**, *43* (12), 2453−2462.

(23) Labedz, O.; Lange, H.; Huczko, A.; Borysiuk, J.; Szybowicz, M.; Bystrzejewski, M. Influence of carbon structure of the anode on the synthesis of single-walled carbon nanotubes in a carbon arc plasma. *Carbon* **2009**, *47* (12), 2847−2854.

(24) Nishizaka, H.; Namura, M.; Motomiya, K.; Ogawa, Y.; Udagawa, Y.; Tohji, K.; Sato, Y. Influence of carbon structure of the anode on the production of graphite in single-walled carbon nanotube soot synthesized by arc discharge using a Fe-Ni-S catalyst. *Carbon* **2011**, *49* (11), 3607−3614.

(25) Zhong, R.; Cong, H. T.; Liu, C. Fabrication of single-walled carbon nanotubes from multi-walled carbon nanotubes and carbon fibers. *Carbon* **2002**, *40* (15), 2970−2973.

(26) Qiu, J. S.; Li, Y. F.; Wang, Y. P.; Wang, T. H.; Zhao, Z. B.; Zhou, Y.; Li, F.; Cheng, H. M. High-purity single-wall carbon nanotubes synthesized from coal by arc discharge. *Carbon* **2003**, *41* (11), 2170−2173.

(27) Qiu, J. S.; Chen, G.; Li, Z. T.; Zhao, Z. B. Preparation of double-walled carbon nanotubes from fullerene waste soot by arc-discharge. *Carbon* **2010**, *48* (4), 1312−1315.

(28) Kanai, M.; Koshio, A.; Shinohara, H.; Mieno, T.; Kasuya, A.; Ando, Y.; Zhao, X. High-yield synthesis of single-walled carbon nanotubes by gravity-free arc discharge. *Appl. Phys. Lett.* **2001**, *79* (18), 2967−2969.

(29) Howard, J. B.; McKinnon, J. T.; Makarovsky, Y.; Lafleur, A. L.; Johnson, M. E. Fullerenes C60 and C70 in flames. *Nature* **1991**, *352* (6331), 139−141.

(30) Egashira, M.; Okada, S.; Korai, Y.; Yamaki, J.; Mochida, I. Toluene-insoluble fraction of fullerene-soot as the electrode of a double-layer capacitor. *J. Power Sources* **2005**, *148*, 116−120.

(31) Spassova, I.; Khristova, M.; Nickolov, R.; Mehandjiev, D. Novel application of depleted fullerene soot (DFS) as support of catalysts for low-temperature reduction of NO with CO. *J. Colloid Interface Sci.* **2008**, *320* (1), 186−193.

(32) Sun, C. H.; Lu, G. Q.; Cheng, H. M. Simple approach to estimating the van der Waals interaction between carbon nanotubes. *Phys. Rev. B* **2006**, *73*(19).

(33) Dresselhaus, M. S.; Dresselhaus, G.; Saito, R.; Jorio, A. Raman spectroscopy of carbon nanotubes. *Phys. Rep.* **2005**, *409* (2), 47−99.

(34) Rols, S.; Righi, A.; Alvarez, L.; Anglaret, E.; Almairac, R.; Journet, C.; Bernier, P.; Sauvajol, J. L.; Benito, A. M.; Maser, W. K.; Munoz, E.; Martinez, M. T.; de la Fuente, G. F.; Girard, A.; Ameline, J. C. Diameter distribution of single wall carbon nanotubes in nanobundles. *Eur. Phys. J. B* **2000**, *18* (2), 201−205.

(35) Sen, R.; Suzuki, S.; Kataura, H.; Achiba, Y. Growth of single-walled carbon nanotubes from the condensed phase. *Chem. Phys. Lett.* **2001**, *349* (5−6), 383−388.

(36) Kataura, H.; Kumazawa, Y.; Maniwa, Y.; Ohtsuka, Y.; Sen, R.; Suzuki, S.; Achiba, Y. Diameter control of single-walled carbon nanotubes. *Carbon* **2000**, *38* (11−12), 1691−1697.
(37) Zhang, Y.; Iijima, S. Formation of single-wall carbon nanotubes by laser ablation of fullerenes at low temperature. *Appl. Phys. Lett.* **1999**, *75* (20), 3087−3089.